Sensors and Materials, Vol. 38, No. 2 (2026) 587–592
MYU Tokyo

S & M 4326

Characterization of Radiophotoluminescence Properties of Eu-doped $Ca_2P_2O_7$

Miho Aoki,[1*] Hidehito Nanto,[1,2] and Go Okada[1]

[1]Co-creative Research Center of Industrial Science and Technology, Kanazawa Institute of Technology, 3-1 Yatsukaho, Hakusan, Ishikawa 924-0838, Japan
[2]Oarai Research Center, Chiyoda Technol Corporation, 3681 Narita-cho, Oarai-machi, Higashi-ibaraki-gun, Ibaraki 311-1313, Japan

(Received October 15, 2025; accepted December 11, 2025)

Keywords: radiophotoluminescence, RPL, Eu, $Ca_2P_2O_7$, dosimeter

Eu-doped $Ca_2P_2O_7$ was synthesized by a solid-state reaction method, and its radiophotoluminescence (RPL) properties were evaluated. Upon X-ray irradiation, an emission from Eu^{2+}, which is not present before irradiation, is observed. The latter photoluminescence (PL) intensity around 375–475 nm increases with dose, and the estimated lower detection limit of radiation dose using this signal is approximately 1 Gy. The dose response relationship follows the following equation: $Response = 6519.5\ Dose^{0.6}$. The signal is stable with only about 0.7% of deviation over 20 min after irradiation, indicating high stability. Furthermore, the signal is strongly affected by thermal treatment at high temperatures, which allows the Eu^{2+} signal to be partially eliminated.

1. Introduction

Radiation is widely utilized in various fields such as medicine and energy.[1] However, excessive exposure to radiation can have severe effects on the human body.[2] Therefore, the development of accurate and reliable dosimetry techniques is of critical importance. Traditionally, thermally stimulated luminescence (TSL)[3,4] and optically stimulated luminescence (OSL)[5,6] have been commonly used for radiation dosimetry.

Radiophotoluminescence (RPL) is a phenomenon in which luminescent centers generated by radiation exposure emit light upon optical excitation. RPL offers the advantage of nondestructive and repeatable readout, making it a promising technique for high-precision dosimetry.[7–9]

Among the reported RPL materials, Ag-doped phosphate glass[10–12] is the most representative and has already been put into practical use. Other common materials include LiF[13] and Al_2O_3:C,Mg.[14] Furthermore, recent studies have expanded the range of RPL materials, such as Sm-doped,[15,16] Eu-doped,[17,18] Bi-doped,[19] as well as undoped materials,[20] being reported as new options. Despite its potential, the development of RPL materials remains in its early stages, with significantly fewer studies compared with TSL and OSL,[9,21] indicating considerable room for the exploration of new materials.

*Corresponding author: e-mail: c6501884@st.kanazawa-it.ac.jp
https://doi.org/10.18494/SAM6001

ISSN 0914-4935
https://myukk.org/

In this study, calcium phosphates were selected as the base materials,[22] and a screening investigation was conducted on 54 samples. These samples were prepared by doping various impurities into matrices containing two or three crystalline phases to evaluate the presence or absence of RPL. As a result, a pronounced RPL response was observed in Eu-doped $Ca_2P_2O_7$. In this paper, we report on the synthesis of $Ca_2P_2O_7$:Eu and its RPL characteristics.

2. Materials and Methods

Eu-doped $Ca_2P_2O_7$ was synthesized via a conventional solid-state reaction. $CaCO_3$ (99.99%, Kojundo Chemical Laboratory), $NH_4H_2PO_4$ (99.999%, Sigma-Aldrich), and Eu_2O_3 (99.9%, Kojundo Chemical Laboratory) were used as the starting materials. These were mixed in stoichiometric ratios corresponding to $(Ca_{1-x}Eu_x)_2P_2O_7$ (x = 0.0002, 0.0005, 0.001, 0.002, 0.005, and 0.01). Moreover, the raw materials were weighed on an electronic balance to make a total weight of 3 g, mixed with a mortar and pestle for 20 min. The thoroughly mixed powder was placed in an alumina crucible. The crucible was next placed in an electric furnace (FT-101FMW, FULL-TECH) and then sintered at 900 °C for 4 h in air. The obtained material was reground, and the following characterizations were conducted in powder form. To evaluate various properties of RPL, the TSL/OSL/RPL Automated and Integrated Measurement System (TORAIMS) was used.[23] While detailed specifications are available elsewhere, a brief overview is provided here. TORAIMS comprises an X-ray generator (XP0758R0, JOB), a Xe lamp (LAX-C100, Asahi Spectra), a multichannel spectrometer (QEPro, Ocean Optics), and an AlN ceramic heater (WALN-3H, Sakaguchi). For PL measurement, the sample was excited through a 310 nm band-pass filter (HMX0310, Asahi Spectra), while the emission spectrum was detected through a 350 nm short-cut filter (LUX350, Asahi Spectra). Moreover, the sample holder used during measurements is circular, with an area of approximately 0.25π cm^2 and a depth of 0.8 mm. The holder is filled with the sample, and the amount employed for a single measurement is about 40 mg. The use of the TORAIMS enables the streamlined and consistent acquisition of luminescence data. RPL signals can be measured sequentially under controlled conditions, allowing for the comprehensive and reproducible characterization of the sample response.

3. Results and Discussion

Figure 1(a) shows the excitation and photoluminescence (PL) spectra of a 0.2% Eu-doped $Ca_2P_2O_7$ sample as a function of X-ray irradiation dose. Before X-ray irradiation, sharp emission peaks were observed at approximately 590 nm ($^5D_0 \rightarrow {}^7F_1$), 610 nm ($^5D_0 \rightarrow {}^7F_2$), 650 nm ($^5D_0 \rightarrow {}^7F_3$), and 695 nm ($^5D_0 \rightarrow {}^7F_4$), attributed to the intra-4f transitions of Eu^{3+}.[24] After X-ray irradiation, an additional broad emission peak was observed around 375–475 nm. Owing to both the PL and excitation spectral features, the emission origin is considered due to the 5d-4f transition of Eu^{2+}. In addition, the emission intensities of Eu^{3+} seem to decrease with increasing dose. Therefore, the observation indicates that the X-ray irradiation reduces the valence state of the Eu^{3+} ion into Eu^{2+}. It is considered that some of the X-ray-generated electrons are captured

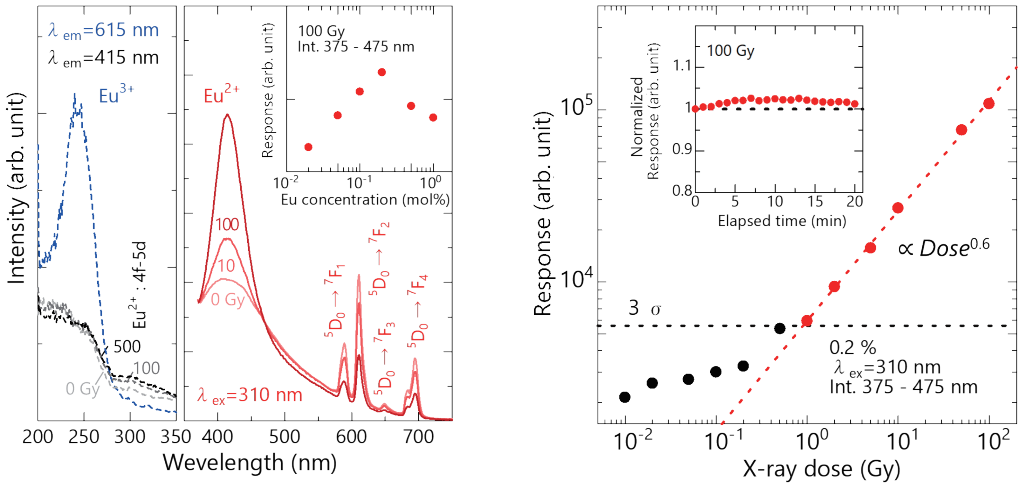

Fig. 1. (Color online) (a) PL emission spectra before and after irradiation at 10 and 100 Gy, and excitation spectra of Eu^{2+} before and after irradiation at 100 and 500 Gy as well as that of Eu^{3+}. The inset compares the sensitivity of RPL as a function Eu concentration. (b) Dose response function of RPL in Eu-doped $Ca_2P_2O_7$. The inset shows a relative RPL response as a function of elapsed time after X-ray irradiation.

by Eu^{3+}, leading to the formation of Eu^{2+}. Simultaneously, an equivalent number of X-ray-generated holes are expected to be trapped at hole-trapping centers. The inset compares the sensitivity of RPL as a function of the concentration of Eu. Here, the RPL response is defined as the integrated PL intensity in the emission region of Eu^{2+} (375–475 nm). It is shown that the sensitivity depends on the concentration of Eu, and the sensitivity is the highest when the concentration is 0.2%.

Figure 1(b) shows the dose response properties. From the intersection with the 3σ line, the lowest detection limit is estimated to be approximately 1 Gy. Even after irradiation up to 100 Gy, no saturation behavior is observed. On the basis of these observations, the response curve within the effective dynamic range is well approximated as $Response = 6519.5\ Dose^{0.6}$. The inset shows the results of the stability evaluation. Compared with Ag-doped phosphate glass, the present material exhibits the lowest detection limit that is approximately 300 times higher.[25] However, whereas the former is known to saturate at doses above 15 Gy, the present material maintains a linear response up to much higher doses, reaching 100 Gy. The evaluation method involved measuring the luminescence intensity at regular intervals (60 s) over a period of 20 min to determine whether the luminescence centers formed by X-ray irradiation are stably retained. The measurements were performed at room temperature. It is shown that the intensity slightly changes with time after irradiation. In the first 10 min, it shows a slight increase in response by approximately 2%, which is considered to be due to the formation of additional luminescent centers. The subsequent decrease in response is attributed to the reduction in the number of luminescent centers. Overall, these changes are minimal, indicating that the PL intensity is essentially stable at room temperature within the tested timeframe. In contrast, Ag-doped phosphate glass has been reported to exhibit a signal increase of approximately 30% at 20 min after X-ray irradiation under identical experimental conditions using TORAIMS.[25]

Consequently, the present material offers a distinct advantage for applications requiring real-time dose measurement.

Figure 2(a) shows the relationship between the annealing temperature and the emission spectrum. Upon thermal treatment, a new emission band centered around 510 nm appears. The intensity of this band increases up to 250 °C, decreases until 400 °C, and then increases again to 500 °C. Given its broad peak shape and presence in the undoped material (not shown), this emission band is considered to originate from defect centers in the host material. The inset shows the integrated PL intensity between 375 and 475 nm. It is illustrated that the intensity strongly increases with temperature up to 225 °C, and it strongly decreases at higher temperatures. The result predominantly reflects the behavior of luminescence by the defect center rather than the Eu^{2+} emission as these two bands strongly overlap each other, although the focus here is on how the Eu^{2+} emission spectrum changes with temperature. To estimate the contribution of the Eu^{2+} emission band at each treatment temperature, the broad defect-related emission between 375 and 475 nm was approximated as a straight line. The area corresponding to the Eu^{2+} emission was then numerically extracted, as illustrated in the inset of Fig. 2(b). The resulting value as a function of treatment temperature is shown in Fig. 2(b). After treatment at 75 °C, the signal shows a slight increase compared with that at 40 °C. This behavior is consistent with the slight increase observed at room temperature following X-ray irradiation [see the inset of Fig. 1(b)]. Therefore, the slight increase at room temperature is attributed to the formation of additional Eu^{2+} centers. As the temperature increases, the emission intensity gradually decreases. However, it remains nearly constant above 350 °C, indicating that the luminescent centers are not completely eliminated. Note that the RPL of Ag-doped phosphate glass can be reversed by treatment at 400 °C for 1 h. In contrast, the present material may require a higher temperature for reversal or the signal may remain irreversible.

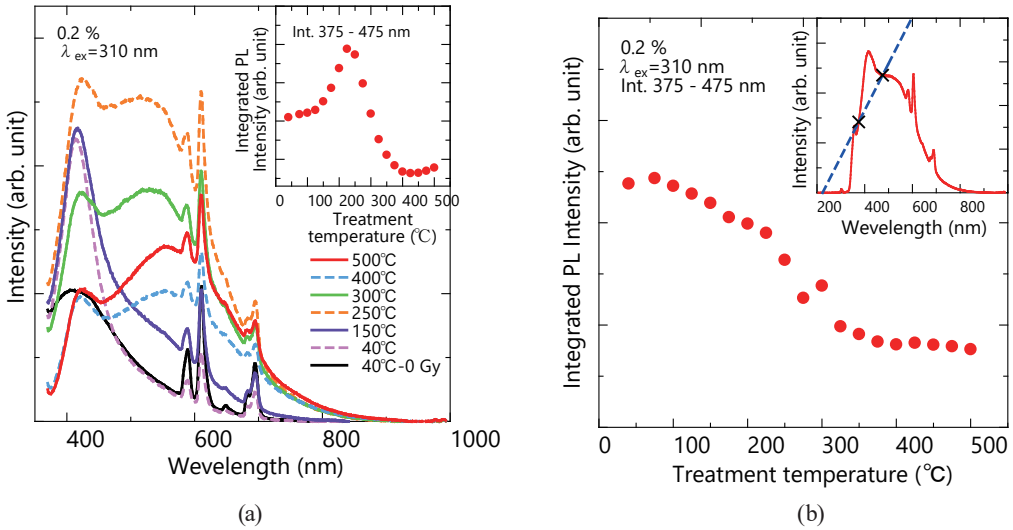

(a) (b)

Fig. 2. (Color online) (a) Dependence of PL spectrum after X-ray irradiation (100 Gy) on thermal treatment temperature from 75 to 500 °C. The inset shows the variation in PL intensity within the Eu^{2+} emission band range (375–475 nm). (b) Temperature dependence of extracted PL intensity of the Eu emission band. The inset shows an example of the extraction process, where the red line represents the measured spectrum and the dashed blue line indicates the baseline.

4. Conclusions

Eu-doped $Ca_2P_2O_7$ phosphors were synthesized via a solid-state reaction, forming a stable single-phase structure. Radiation-induced $Eu^{3+} \rightarrow Eu^{2+}$ conversion enables a strong RPL response with the lowest detection limit of 1 Gy. No saturation is confirmed up to 100 Gy, and the signal remains stable over time. The signal is strongly affected by thermal treatment at high temperatures, which allows the Eu^{2+} signal to be partially eliminated.

Acknowledgments

This work was supported by a Grant-in-Aid for Scientific Research (B) (22H02009) from the Ministry of Education, Culture, Sports, Science and Technology of Japan (MEXT), Shibuya Science Culture and Sports Foundation, as well as the Research Center for Biomedical Engineering. Also, part of this work was performed as a joint research with the Nuclear Power Safety Technology Research Center of Chubu Electric Power Co., Inc.

References

1 M. Donya, M. Radford, A. ElGuindy, D. Firmin, and M. H. Yacoub: Global Cardiol. Sci. Pract. **2014** (2014) 57. https://doi.org/10.5339/gcsp.2014.57
2 J. Talapko, D. Talapko, D. Katalinić, I. Kotris, I. Erić, D. Belić, M. Vasilj Mihaljević, A. Vasilj, S. Erić, J. Flam, S. Bekić, S. Matić, and I. Škrlec: Medicina **60** (2024) 653. https://doi.org/10.3390/medicina60040653
3 K. Shinsho: Phosphors for Radiation Detectors, T. Yanagida and M. Koshimizu, Eds. (John Wily & Sons Ltd., Croydon, 2022) 1st ed., Chap. 7. https://doi.org/10.1002/9781119583363.ch7
4 M. Martini and F. Meinardi: Riv. Nuovo Cimento **20** (1997) 1. https://doi.org/10.1007/BF02897907
5 E. G. Yukihara and S. W. McKeever: Phys. Med. Biol. **53** (2008) 181. https://doi.org/10.1088/0031-9155/53/20/R01
6 L. Yuan, Y. Jin, Y. Su, H. Wu, Y. Hu, and S. Yang: Laser Photonics Rev. **14** (2020) 2000123. https://doi.org/10.1002/lpor.202000123
7 G. Okada: Phosphors for Radiation Detectors, T. Yanagida and M. Koshimizu, Eds. (John Wily & Sons Ltd., Croydon, 2022) 1st ed., Chap. 9. https://doi.org/10.1002/9781119583363.ch9
8 J. A. Perry: RPL Dosimetry (IOP Publishing, Bristol, 1987).
9 G. Okada, T. Yanagida, H. Nanto, and S. Kasap: J. Ceram. Soc. Jpn. **129** (2021) 419. https://doi.org/10.2109/jcersj2.21056
10 H. Nanto, Y. Miyamoto, Y. Takei, K. Hirasawa, and K. Endo: Proc. 2013 IEEJ 133rd Trans. Sensors and Micromachines (IEEJ, 2013) 307−311. https://doi.org/10.1541/ieejsmas.133.307
11 T. Kurobori, W. Zheng, Y. Miyamoto, H. Nanto, and T. Yamamoto: Opt. Mater. **32** (2010) 1231. https://doi.org/10.1016/j.optmat.2010.04.004
12 H. Masai, Y. Yanagida, H. Kawamoto, Y. Koguchi, M. Koshimizu, and M. Yamawaki: Sens. Mater. **34** (2022) 699. https://doi.org/10.18494/SAM3688
13 M. Levita and S. Tuvya: IEEE Trans. Nucl. Sci. **23** (1976) 667. https://doi.org/10.1109/TNS.1976.4328325
14 M. S. Akselrod and A. E. Akselrod: Radiat. Prot. Dosim. **119** (2006) 218. https://doi.org/10.1093/rpd/nci663
15 J. Qiu and K. Hirao: J. Mater. Sci. Lett. **20** (2001) 691. https://doi.org/10.1023/A:1010998605695
16 G. Belev, G. Okada, D. Tonchev, C. Koughia, C. Varoy, A. Edgar, T. Wysokinski, D. Chapman, and S. Kasap: Phys. Status Solidi C. **8** (2011) 2822. https://doi.org/10.1002/pssc.201084103
17 H. Ito, G. Okada, Y. Koguchi, W. Kada, K. Watanabe, and H. Nanto: Sens. Mater. **36** (2024) 559. https://doi.org/10.18494/SAM4765
18 S. Asada, G. Okada, T. Kato, F. Nakamura, N. Kawano, N. Kawaguchi, and T. Yanagida: Chem. Lett. **47** (2018) 59. https://doi.org/10.1246/cl.170940
19 G. Okada, C. P. Fernandes, H. Ito, Y. Koguchi, S. Ueno, C. Sawai, W. Kada, K. Watanabe, K. Shinsho, and H. Nanto: Sens. Mater. **37** (2025) 533. https://doi.org/10.18494/SAM5440

20 G. Okada, Y. Koguchi, T. Yanagida, and H. Nanto: Mater. Today Commun. **24** (2020) 101013. https://doi.org/10.1016/j.mtcomm.2020.101013
21 G. Okada, Y. Koguchi, T. Yanagida, S. Kasap, and H. Nanto: Jpn. J. Appl. Phys. **62** (2023) 010609. https://dx.doi.org/10.35848/1347-4065/ac9023
22 T. Goto and H. Katsui: Interface Oral Health Science 2014, K. Sasaki, O. Suzuki, and N. Takahashi, Eds. (Springer, Tokyo, 2015) Chap. 9. https://doi.org/10.1007/978-4-431-55192-8_9
23 G. Okada, K. Hirasawa, T. Yanagida, and H. Nanto: Sens. Mater. **33** (2021) 2117. https://doi.org/10.18494/SAM.2021.3327
24 L. Zhou, P. Du, and L. Li: Sci. Rep. **10** (2020) 20180. https://doi.org/10.1038/s41598-020-77185-w
25 G. Okada, W. Shinozaki, S. Ueno, Y. Koguchi, K. Hirasawa, F. d'Erriko, T. Tanagida, S. Kasap, and H. Nanto: Jpn. J. Appl. Phys. **61** (2022) 1035. https://iopscience.iop.org/article/10.35848/1347-4065/ac1ab2